Heterocyclic Letters
Vol. 14| No.2|273-286|Feb-April|2024
ISSN : (print) 2231–3087 / (online) 2230-9632
CODEN: HLEEAI
http://heteroletters.org

PHYSICOCHEMICAL PARAMETERS INVOLVED IN THE INTERACTION OF SOME PHENANTHROLINE DERIVATIVES WITH JANUS KINASE-3 PROTEIN USING A THEORETICAL MODEL

Rosas-Nexticapa Marcela[1], Figueroa-Valverde Lauro[2*], López-Ramos Maria[2], Alvarez-Ramirez Magdalena[1], Hernández-Vazquez Patricia[1], Cauich-Carrillo Regina[3], Mijangos-Sanchez Julliete[2].

[1]Laboratory of Pharmaco-Chemistry, Faculty of Chemical Biological Sciences, University Autonomous of Campeche, Av. Agustín Melgar s/n, Col Buenavista C.P. 24039 Campeche, Camp., México.
[2]Facultad de Nutrición, Universidad Veracruzana, Médicos y Odontologos s/n C.P. 91010, Unidad del Bosque Xalapa Veracruz, México.
[3] University Autonomous of Quintana Roo State, Campus Chetumal, Av Erik Paolo Martinez s/n esq. Av. 4 de marzo, Col. Magisteterial, C.P. 77039, México
** Correspondence: lfiguero@uacam.mx*

ABSTRACT

Several phenanthroline derivatives have been synthesized as anticancer agents; however, the physicochemical properties involved in the interaction of phenanthroline derivatives with some biomolecules involved in cancer cells, such as the Janus Kinase-3 protein, are not clear. Analyzing these data, in this study some pharmacophores were developed for phenanthroline derivatives (1-22) using LigandScout software. Besides, some physicochemical parameters such as HBD (hydrogen bond donor), HBA (hydrogen bond acceptor), HOMO (highest occupied molecular orbital), and LUMO (lowest unoccupied molecular orbital) were analyzed using Spartan software.

On the other hand, some thermodynamic parameters involved in the interaction between phenanthroline derivatives and Janus Kinase-3 protein, such as inhibition constant (Ki), were determined using decernotinib and tofacitinib as controls in the DockingServer program. The results showed several pharmacophore models for compounds 1-22, which involve different HBA or HBD groups. Other data involved in phenanthroline derivative-protein complex formation displayed that Ki values for compounds 1, 6, and 8 were lower compared with 2-5, 7, 9, and 11-22. Finally, Ki was lower for 22 compared with decernotinib; in addition, Ki for 22 was similar compared with tofacitinib. All these results indicate that compound 22 could decrease cancer cells, and this phenomenon could depend on its physicochemical characteristics.

KEYWORDS. Phenanthroline, derivatives, hydrogen bond acceptor, hydrogen bond donor, Janus Kinase-3

INTRODUCTION

For several years, the synthesis of heterocyclic compounds with biological activity has been of great interest in both the organic chemistry and pharmacy fields[1-iv]. For example, the synthesis and evaluation of the anti-inflammatory activity of some phenothiazine derivatives[v]. Another report displayed the antibacterial activity of heterocyclic derivatives containing sulfonyl or sulfonamide and their structure-activity evaluation[vi]. Besides, other studies on structure-activity have shown that a heterocyclic-imidazol derivative may have biological activity against cancer using a theoretical model[vii]. Another report showed the structure-activity relationships for benzimidazol-2-ylidene derivative N-heterocyclic-carbene complexes as anticancer agents[viii]. Furthermore, a study displayed the structure-activity relationship of some imine-N-heterocyclic carbene ruthenium (II) complexes using A549 cancer cells[ix].

On the other hand, there are some studies that indicate that other types of heterocyclic, such as phenanthroline and its derivatives, can produce biological activity in cancer cells. For example, a report showed the preparation of 1,10-phenanthroline and some 1,10-phenanthroline Cooper derivatives, which decreased cancer using A-498 and Hep-G2 cell lines[x]. Other studies displayed that the salicylate-phenanthroline-copper (II) complex decreased growth cancer using MDA-MB-231 and BT-20 cell lines[xi]. Besides, a report showed the synthesis of a phenanthroimidazole derivative as an anticancer agent using a human esophageal tumor cell line (Eca-109)[xii]. In addition, a glucose-curcumin-biotinylated 1,10-phenanthroline complex was prepared with biological activity against human breast cancer MDA-MB 231[xiii]. Another study displayed the preparation of Cu(benzim)2(phen)(MeOH)](ClO4)2 complex with biological activity on the cisplatin-resistant breast cancer cell line (HCC1428)[xiv]. Furthermore, an experimental and theoretical study demonstrated the synthesis of the compound ethyl 11-(3,4-dimethoxybenzoyl)pyrrolo[1,2-a][1,10]phenanthroline-9-carboxylate as an anticancer agent against the colorectal cancer cell line (COLO205); it is noteworthy that this study suggests that interaction with the tubulin surface could be via a hydrogen bond with the Asn101 aminoacid residue[xv]. Besides, a 3-indolepropionic acid-Copper II-phenanthroline complex was synthesized as an anticancer agent against MCF-7 breast cancer cells, and their possible interaction with a proteosome was determined using a theoretical model[xvi]. All these data suggest that several phenanthroline derivatives can decrease the biological activity of some cancer strains; however, their chemical interaction with some biomolecules responsible for producing cancer is very confusing. To analyze these, the aim of this study was to evaluate the possible interaction of twenty-two phenanthroline derivatives (Figure 1) with Janus Kinase-3, which is involved in cancer cell growth, using some theoretical models.

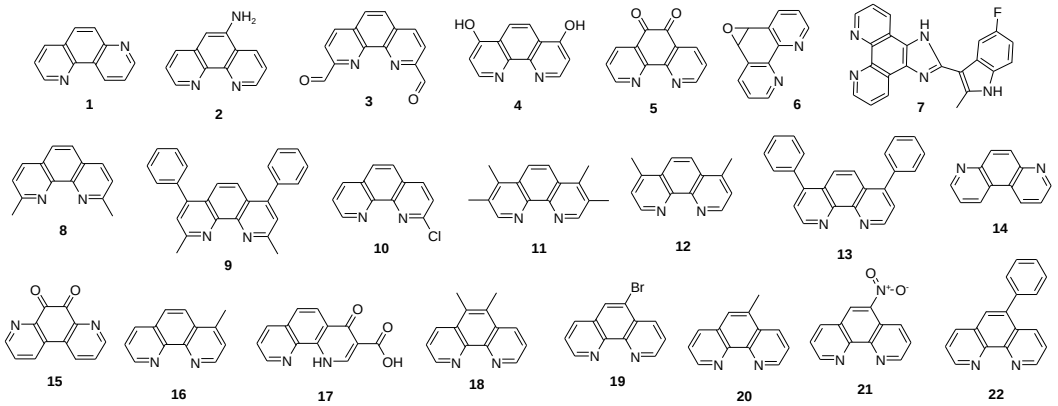

Figure 1, Chemical structure of phenanthroline derivatives (1-22)

1 = 1,7-Phenanthroline
2 = 1,10-Phenanthrolin-5-amine
3= 1,10-Phenanthroline-2,9-dicarbaldehyde
4 = 1,10-Phenanthroline-4,7-diol
5 = 1,10-Phenanthroline-5,6-dione
6=1a,9b-Dihydrooxireno[2,3-f][1,10]phenanthroline
7=2-(5-fluoro-2-methyl-1H-indol-3-yl)-1H-imidazo[4,5-f][1, 10]phenanthroline
8 =2,9-Dimethyl-1,10-phenanthroline
9=2,9-Dimethyl-4,7-diphenyl-1,10-phenanthroline
10 = 2-chloro-1,10-phenanthroline
11=3,4,7,8-Tetramethyl-1,10-phenanthroline
12 = 4,7-Dimethyl-1,10-phenanthroline
13 = 4,7-Diphenyl-1,10-phenanthroline
14 = 4,7-Phenanthroline
15 = 4,7-Phenanthroline-5,6-dione
16 = 4-Methyl-1,10-phenanthroline
17=4-oxo-1H-1,10-phenanthroline-3-carboxylic acid
18 = 5,6-Dimethyl-1,10-phenanthroline
19 = 5-Bromo-1,10-phenanthroline
20 = 5-Methyl-1,10-phenanthroline
21 = 5-Nitro-1,10-phenanthroline
22 = 5-Phenyl-1,10-phenanthroline

2. Materials and Methods

2.1 Pharmacophore model.

3D pharmacophore model for phenanthroline derivatives (**1** to **22**) was evaluated using LigandScout 4.08 software[xvii].

2.2 Physicochemical properties

HOMO, LUMO, dipole moment (μ) were determinate using Spartan´16 (v.2.7)[xviii]. The physicochemical parameters $LogP_{O/W}$, TPSA (topological polar surface area) and MR (molar refractory) for phenanthroline derivatives was carried out using SwissAdme[xix].

2.2 Protein-Ligand

The interaction of phenanthroline derivatives (**1** to **22**) with 3pjc (PDB doi:https://doi.org/10.2210/ pdb3PJC/pdb) was determined using decernotinib and tofacitinib as controls in DockingServer program[xx].

2.4 pKa analysis

The pKa for phenanthroline derivatives was determined using Chemaxon program[xxi].

RESULTS AND DISCUSSION

Physicochemical parameters

Several phenanthroline derivatives have been prepared to treat cancer cells[xxii-xxv]; however, the physicochemical properties involved in the interaction with some biomolecules are not clear. Analyzing these data in this study, some physicochemical parameters involved in the coupling of twenty-two phenanthroline derivatives were determined using some theoretical models. The first stage involves the design of some pharmacophore models for each phenanthroline derivative using the LigandScout 4.0 software[xxvi]. It is noteworthy that the pharmacophore model is used to design new molecules with possible biological activity on some biomolecule[xxvii-xxix]. The results (Figures 2 and 3) showed several functional groups involved in the different phenanthroline derivatives, which could act as hydrogen-bonded acceptors (HBA) and hydrogen-bonded donors (HBD) on some biomolecule surfaces. This phenomenon could be translated as a possible interaction of phenanthroline derivatives with some biomolecule, resulting in changes in its biological activity.

Analyzing the hypothesis above mentioned and other data that suggest that molecular orbitals HOMO and LUMO can be used to predict the most reactive position in some electron systems on several types of reactions, which are translated as changes in the biological activity of some compounds[xxx], In this study, both molecular orbitals HOMO and LUMO involved in the chemical structure of phenanthroline derivatives were determined; the results (Figure 4-7, Table 1) showed different HOMO and LUMO values, which could be related to different functional groups bound to the phenanthroline nucleus and different positions of nitrogen's in the phenanthroline nucleus, and this phenomenon could also be conditioned by π orbitals that are localized in the phenanthroline nucleus. Besides, HOMO-LUMO gap values were determinate for phenanthroline derivatives; the results display that values for compounds 1 (10.03), 6 (10.27), and 8 (10.00) were higher compared with 2-5, 7, 9, and 11-22, which could confer higher stability to phenanthroline derivatives.

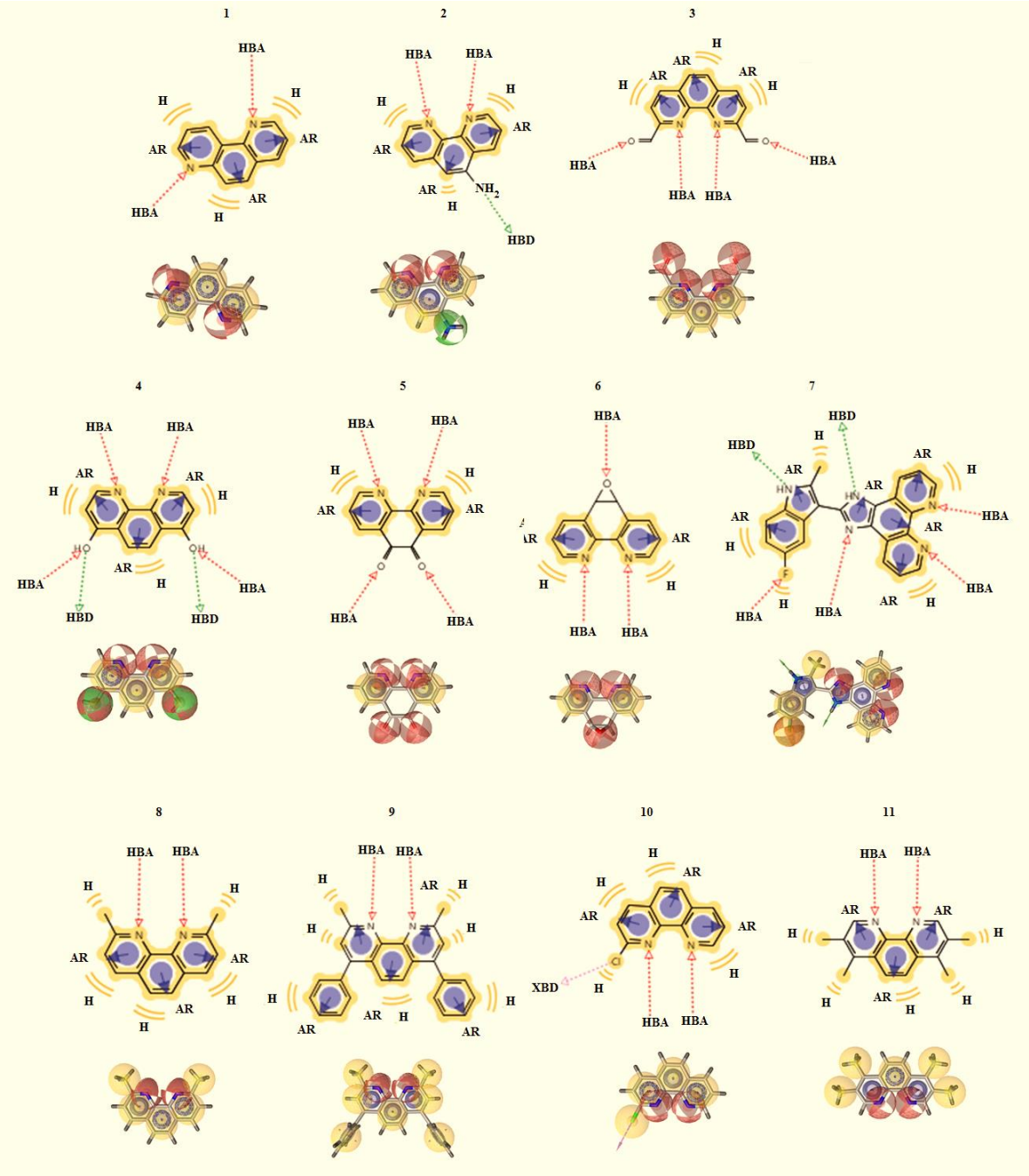

Figure 2. Pharmacophores from phenanthroline derivatives (1-11) using the LigandScout 4.08 program[xviii].
HBA = Hydrogen bond acceptors (red); HBD = Hydrogen bond donors (green).

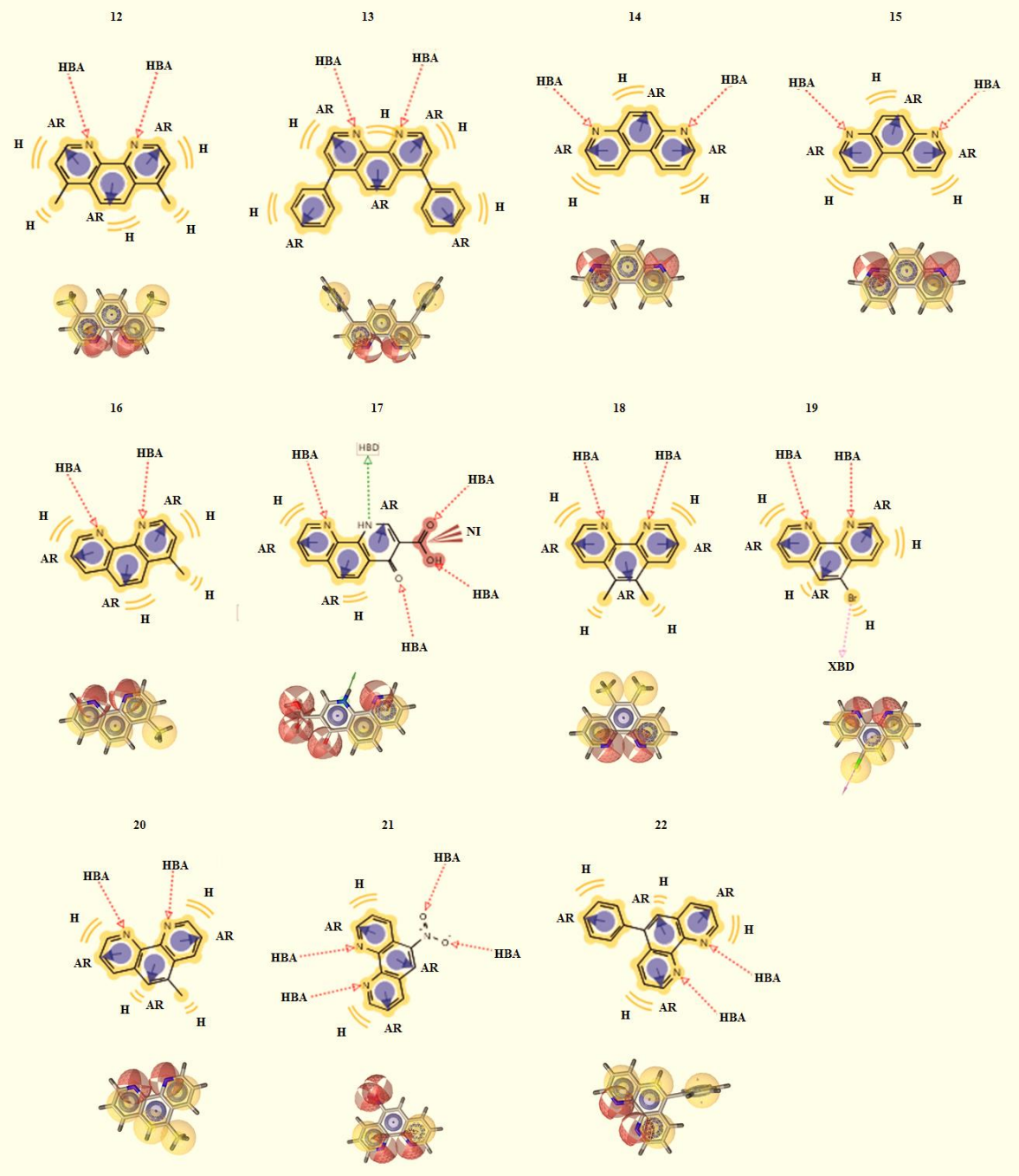

Figure 3. Pharmacophores from phenanthroline derivatives (1-11). Visualized with LigandScout 4.08 program[xviii]. HBA = Hydrogen bond acceptors (red); HBD = Hydrogen bond donors (green); NI =

.

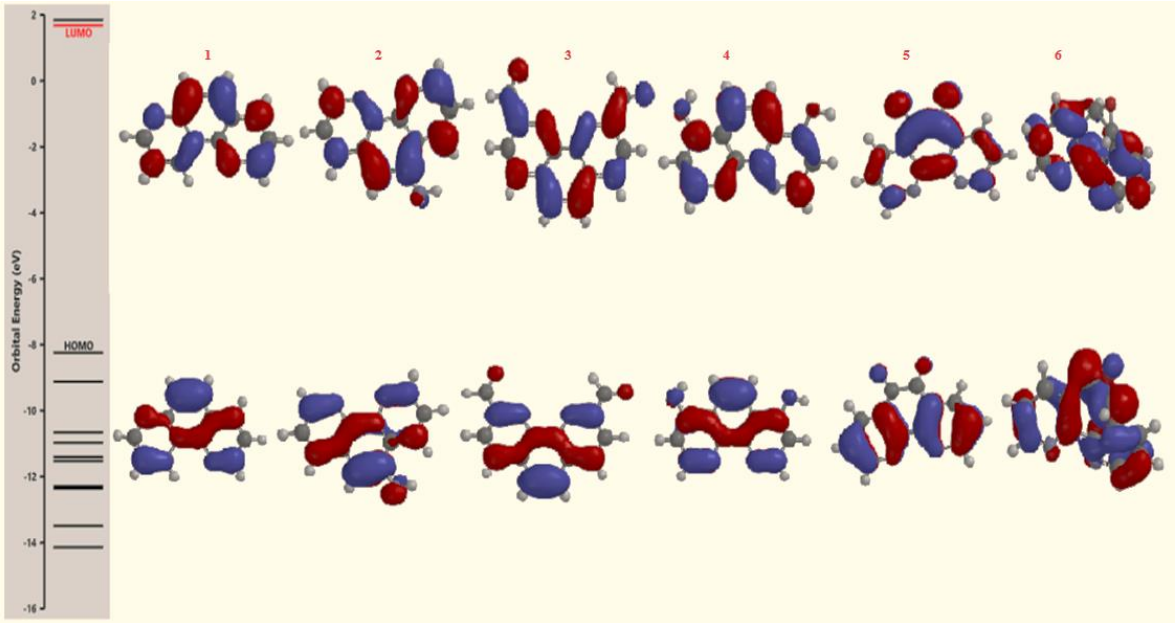

Figure 4. HOMO and LUMO orbitals for phenanthroline derivatives (1-6). Visualized with Sartan-16.0 program.

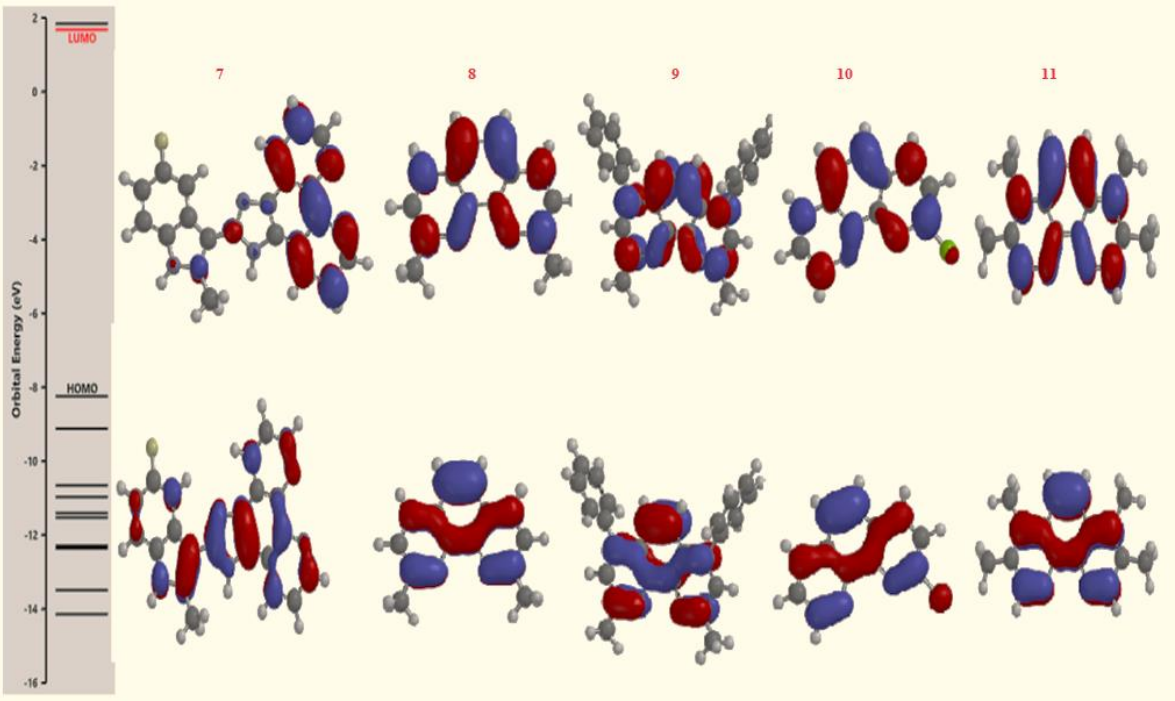

Figure 5. Visualization of HOMO and LUMO orbitals for phenanthroline derivatives (7-10) using Sartan-16.0 program.

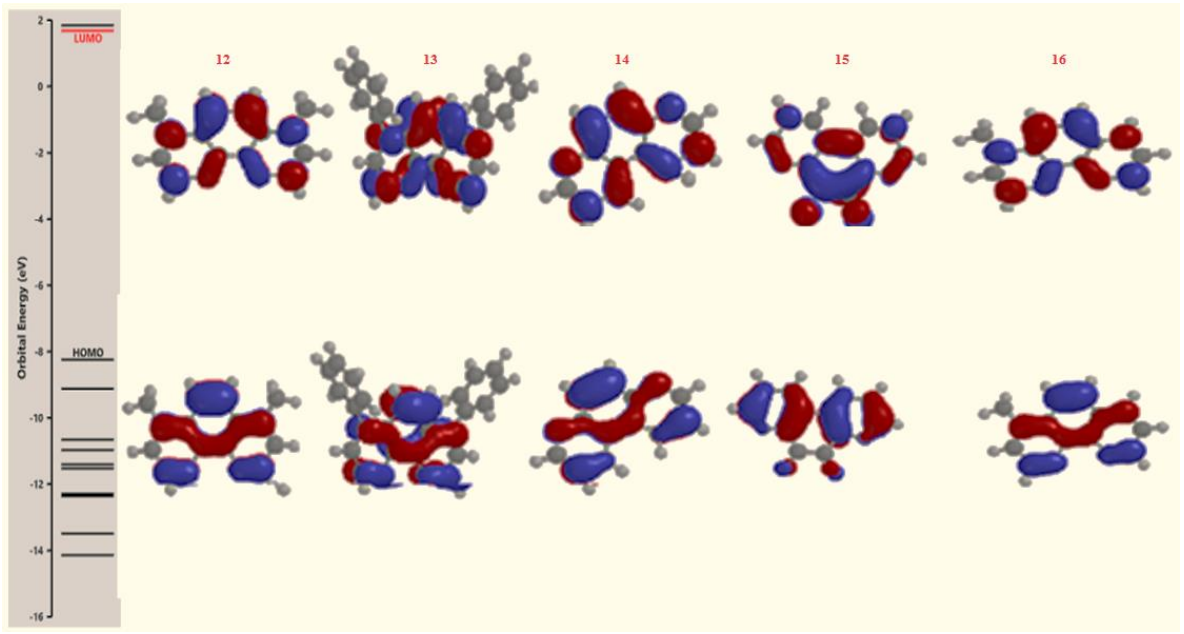

Figure 6. HOMO and LUMO orbitals for phenanthroline derivatives (12-16). Visualized with Sartan-16.0 program.

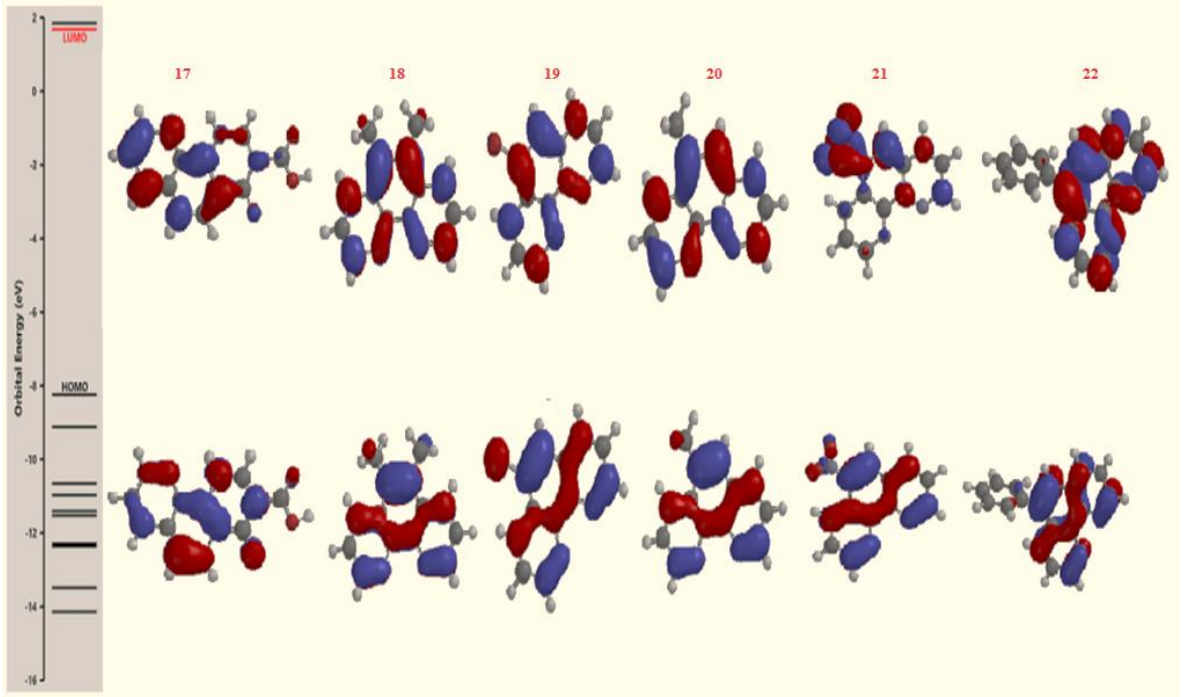

Figure 7. Visualization of HOMO and LUMO orbitals for phenanthroline derivatives (17-22) using Sartan-16.0 program.

Table 1. Physicochemical properties of phenanthroline derivatives (1-22).

Compound	HBA	HBD	HOMO	LUMO	E-gap	μ	MR	TPSA	$LogP_{O/W}$	PKa
1	2	0	-8.20	1.83	10.03	2.33	57.04	25.78	2.42	3.11
2	2	1	-7.32	1.96	9.28	3.65	61.45	51.80	1.78	3.17
3	4	0	-8.68	0.71	9.36	8.82	67.82	59.92	1.75	-0.80
4	4	2	-7.93	2.01	9.94	4.26	61.09	66.24	1.49	-10.04
5	4	0	9.46	0.29	9.75	2.50	56.13	58.82	1.01	-2.65
6	3	0	-8.33	1.94	10.27	1.16	54.26	38.31	1.40	3.82
7	4	2	-7.22	2.13	9.35	10.34	108.91	70.25	4.25	10.72
8	2	0	-7.81	2.19	10.00	2.85	66.98	25.78	3.04	2.45
9	2	0	-7.67	2.19	9.86	3.39	117.85	25.78	5.71	2.50
10	2	0	-8.24	1.68	9.92	5.65	62.05	25.78	2.83	0.64
11	2	0	-7.75	1.97	9.72	4.16	76.91	25.78	3.65	3.06
12	2	0	-7.37	1-94	9.31	4.35	66.98	25.78	3.00	2.59
13	2	0	-7.92	1.97	9.89	4.42	107.92	25.78	5.02	1.85
14	2	0	-8.31	1.69	10.00	3.93	57.04	25.78	2.31	3.38
15	4	0	9.44	0.43	9.87	9.78	56.13	59.92	1.02	1.69
16	2	0	-7.98	1.95	9.93	4.10	62.01	25.78	2.54	2.35
17	4	2	-8.16	1.29	9.45	7.04	66.83	83.05	1.62	6.55
18	2	0	-7.78	2.07	9.80	4.35	66.98	25.78	2.98	2.40
19	2	0	-8.20	1.60	9.80	2.25	64.74	25.78	2.97	0.79
20	2	0	-7.94	2.00	9.94	4.06	62.01	25.78	2.67	2.12
21	4	0	-8.90	0.06	8.96	3.09	65.87	71.60	1.72	-0.40
22	2	0	-8.00	1.94	9.94	4.09	82.48	25.78	3.70	1.69

Ligand-protein complex

Some theoretical studies indicate that some phenanthroline derivatives may interact with some biomolecules involved in some cancer strains; however, this phenomenon is very confusing, perhaps due to the different experimental methods used[xv, xvi].

Analyzing these data, in this investigation, some physicochemical parameters involved in the possible interaction of phenanthroline derivatives with Janus Kinase-3, which is a biomolecule involved in cancer growth[xxxi-xxxiii], were determined using the DockingServer program. Besides, two Janus kinase-3 inhibitors, such as decernotinib[xxxiv] and tofactinib[xxxv], were used as controls. The results showed (Table 2) different amino acid residues in the interaction of phenanthroline derivatives with the 3pjc protein surface compared with the controls. This data could be due to differences in chemical structure, which can be translated as differences in lipophilicity degree (Table 1). However, it is important to mention that other studies suggest that several thermodynamic parameters could condition the interaction of some compounds with different biomolecules.

Table 2. Aminoacid residues involved in the coupling of phenanthroline derivatives (compounds 1-22), decernotinib and tofacitinib with 3pjc protein surface.

Compound	**Aminoacid residues**
Decernotinib	Leu828; Gly829; Phe833; Val836; Lys855;Met902; Cys909; Asp912; Arg953; Asn954; Leu956; Asp967
Tofacitinib	Leu_{828}; Phe_{833}; Val_{836}; Ala_{853}; Lys_{855}; Glu_{871}; Leu_{875}; Leu_{900}; Met_{902}; Tyr_{904};Leu_{956}
1	Phe_{833}; Val_{836}; Lys_{855}; Glu_{871}; Leu_{875}; Val_{884}; Leu_{900}; Met_{902}; Ala_{966}; Asp_{967}
2	Phe_{833}; Lys_{855}; Glu_{871}; Leu_{875}; Val_{884}; Leu_{900}; Met_{902}; Leu_{956}; Ala_{966}; Asp_{967}
3	Leu_{828}; Phe_{833}; Val_{836}; Ala_{853}; Lys_{855}; Met_{902}; Leu_{956}
4	Leu_{828}; Val_{836}; Ala_{853};Tyr_{904}; Leu_{905}; Leu_{956}
5	Leu_{828}; Val_{836}; Ala_{853};Tyr_{904}; Leu_{905}; Leu_{956}
6	Phe_{833}; Val_{836}; Lys_{855}; Glu_{871}; Leu_{875}; Val_{884}; Leu_{900}; Met_{902}; Leu_{956}; Ala_{966}; Asp_{967}
7	Leu_{828}; Phe_{833}; Ala_{853}; Lys_{855}; Glu_{871}; Leu_{875}; Val_{884}; Leu_{900}; Met_{902}; Tyr_{904}; Cys_{909}; Arg_{953}; Leu_{956}; Asp_{967}
8	Phe_{833}; Val_{836}; Lys_{855}; Glu_{871}; Leu_{875}; Val_{884}; Leu_{900}; Met_{902}; Leu_{956}; Ala_{966}; Asp_{967}; Phe_{968}
9	Phe_{833}; Ala_{853}; Lys_{855}; Glu_{871}; Leu_{875}; Val_{884}; Met_{902}; Leu_{956}; Asp_{967}
10	Phe_{833}; Val_{836}; Lys_{855}; Glu_{871}; Leu_{875}; Val_{884}; Leu_{900}; Met_{902}; Arg_{953}; Leu_{956}; Ala_{966}; Asp_{967}
11	Leu_{828}; Val_{836}; Ala_{853}; Lys_{855}; Glu_{871}; Val_{884}; Met_{902}; Tyr_{904}; Leu_{956}; Asp_{967}
12	Leu_{828}; Ala_{853}; Tyr_{904}; Leu_{905}; Leu_{956}
13	Ala_{853}; Met_{902}; Tyr_{904}; Leu_{905}; Leu_{956}; Ala_{966}
14	Phe_{833}; Val_{836}; Lys_{855}; Glu_{871}; Leu_{875}; Val_{884}; Met_{902}; Asp_{967}; Phe_{968}
15	Leu_{828}; Phe_{833}; Val_{836}; Ala_{853}; Tyr_{904}; Leu_{905}; Leu_{956}
16	Leu_{828}; Val_{836}; Ala_{853}; Tyr_{904}; Leu_{905}; Leu_{956}
17	Leu_{828}; Ala_{853}; Tyr_{904}; Leu_{905}; Leu_{956}
18	Leu_{828}; Val_{836}; Ala_{853}; Tyr_{904}; Leu_{905}; Leu_{956}
19	Leu_{828}; Val_{836}; Ala_{853}; Tyr_{904}; Leu_{905}; Leu_{956}
20	Leu_{828}; Val_{836}; Ala_{853}; Tyr_{904}; Leu_{905}; Leu_{956}
21	Leu_{828}; Val_{836}; Ala_{853}; Tyr_{904}; Leu_{905}; Leu_{956}
22	Leu_{828}; Phe_{833}; Val_{836}; Ala_{853}; Glu_{871}; Leu_{875}; Val_{884}; Leu_{900}; Met_{902}; Tyr_{904}; Leu_{956}; Ala_{966}; Phe_{968}

The results showed (Table 2) different amino acid residues in the interaction of phenanthroline derivatives with the 3pjc protein surface compared with the controls. This data could be due to differences in chemical structure, which can be translated as differences in lipophilicity degree (Table 1). However, it is important to mention that other studies suggest that several thermodynamic parameters could condition the interaction of some compounds with different biomolecules[xxxvi].

Thermodynamic parameters

For several years, different computational studies have been developed to predict some thermodynamic parameters involved in ligand-protein complexes formation[xxxvii, xxxviii].

Analyzing the data, in this study some thermodynamic parameters involved in the interaction of phenanthroline derivatives with 3pjc protein surface were determinate using DockingServer program. The results showed displayed differences in the energy levels involved in the interaction of coumarin and its derivatives with 3pjc protein surface compared with both decernotinib and tofacitinib drugs (Table 3). Besides, inhibition constant (Ki) was lower for phenanthroline derivative (compound 22) compared with decernotinib and Ki was similar for tofacitinib.

Table 3. Thermodynamic parameters involved in the interaction of phenanthroline derivatives (compounds 1-22), decernotinib and tofacitinib with 3pjcprotein surface using DockingServer program.

Compound	**A**	**B**	**C**	**D**	**E**	**F**
Decernotinit	-7.49	3.22	-8.24	0.03	-8.22	
Tofacitinib	-7.69	2.30	-8.60	-0.09	-8.69	721.73
1	-6.16	30.52	-6.12	-0.04	-6.16	492.68
2	-6.77	10.97	-7.02	-0.05	-7.06	539.07
3	-6.12	32.40	-6.69	-0.02	-6.70	543.12
4	-5.22	148.52	-5.82	-0.02	-5.84	507.99
5	-6.19	29.12	-6.18	-0.01	-6.19	496.13
6	-6.16	30.46	-6.06	-0.10	-6.16	504.50
7	-8.88	309.50	-9.18	0.01	-9.18	849.13
8	-6.98	7.60	-6.90	-0.08	-6.98	547.06
9	-8.46	629.41	-9.28	-0.02	-9.30	918.21
10	-7.19	5.33	-7.12	-0.08	-7.19	519.38
11	-7.23	5.04	-7.21	-0.02	-7.23	616.93
12	-6.84	17.79	-6.47	-0.01	-6.48	546.64
13	-8.75	386.18	-9.34	-0.01	-9.35	875.81
14	-6.14	31.32	-6.22	0.08	-6.14	488.68
15	-6.06	36.24	-6.09	0.03	-6.06	496.86
16	-6.23	27.11	-6.22	-0.01	-6.23	523.83
17	-6.15	31.10	-6.57	0.12	-6.45	523.18
18	-6.67	12.84	-6.66	-0.01	-6.67	602.49
19	-6.43	19.22	-6.43	-0.01	-6.43	476.38
20	-6.30	23.94	-6.30	0.00	-6.30	505.25
21	-6.75	11.19	-7.05	0.00	-7.05	513.86
22	-7.63	2.54	-7.93	0.00	-7.93	646.80

A = Est: Free Energy of Binding (kcal/mol); B = Inhibition Constant, Ki (mM); C = vdW + Hbond + desolv Energy (kcal/mol); D = Electrostatic Energy (kcal/mol); E = Total Intermolec. Energy (kcal/mol); F = Interact. Surface

CONCLUSION

This theoretical study suggests that several physicochemical parameters could be involved in the interaction of phenanthroline derivatives with JAK-3 protein, such as different functional groups (which may act as hydrogen-bonded acceptors or hydrogen-bonded donors), lipophilicity degree (LogP), and some thermodynamic factors that could condition the biological activity of JAK-3. In this way, the results indicated that the phenanthroline

derivative (compound 22) could decrease cancer growth. This data suggests that this phenanthroline derivative could be considered a good anticancer agent; however, it is important to mention that other types of biological experiments could be carried out to confirm this hypothesis.

ACKNOWLEDGEMENT
None

CONFLICT OF INTEREST
Authors declare that there is no conflict of interests regarding the publication of the paper.

REFERENCES

i Obaid R.; Mughal E.; Naeem N.; Al-Rooqi M.; Sadiq A.; Jassas R.; Ahmed S.; Pharmacological significance of nitrogen-containing five and six-membered heterocyclic scaffolds as potent cholinesterase inhibitors for drug discovery; Proc. Biochem.; 2022, **120**, 250.

Ii Ali M.; Naseer M.; Recent biological applications of heterocyclic hybrids containing s-triazine scaffold; *RSC Advances*; 2023, **13** (43), 30462.

iii Hou W.; Xu H.; Incorporating selenium into heterocycles and natural products-from chemical properties to pharmacological activities; J. Med. Chem.; 2022, **65**(6), 4436.

iv Nagaraja O.; Bodke Y.; Thippeswamy B.; Venkatesh T.; Manjunatha B.; Synthesis, characterization and biological evaluation of heterocyclic compounds containing 4-methylumbelliferone; J. Mol. Struc.; 2022, **1269**, 133759.

v Sharma S.; Srivastava, V.; Kumar, A.; Synthesis and anti-inflammatory activity of some heterocyclic derivatives of phenothiazine; J. Pharm. Sci.; 2005, **60**(1), 18.

vi Verma S.; Verma, R.; Xue, F.; Thakur, P.; Girish, Y.; Rakesh, K.; Antibacterial activities of sulfonyl or sulfonamide containing heterocyclic derivatives and its structure-activity relationships (SAR) studies: A critical review; Bioorg. Chem.; 2020, **105**, 104400.

vii Nada H.; Elkamhawy, A.; Lee, K.; Structure activity relationship of key heterocyclic anti-angiogenic leads of promising potential in the fight against cancer; Molecules, 2021, **26**(3), 553.

viii Lam N.; Truong D.; Burmeister H.; Babak M.; Holtkamp H.; Movassaghi S.; Hartinger, C.; From catalysis to cancer: Toward structure–activity relationships for benzimidazol-2-ylidene-derived N-heterocyclic-carbene complexes as anticancer agents; Inorg. Chem.; 2018, 57(22), 14427.

ix Yang Y.; Guo, L.; Tian, Z.; Liu, X.; Gong, Y.; Zheng, H.; Liu, Z.; Imine-N-Heterocyclic Carbenes as Versatile Ligands in Ruthenium (II) p-Cymene Anticancer Complexes: A Structure–Activity Relationship Study; Chemistry-An Asian J.; 2018, **13**(19), 2923.

x Deegan C.; McCann M.; Devereux M.; Coyle B.; Egan, D.; In vitro cancer chemotherapeutic activity of 1, 10-phenanthroline (phen),[Ag2 (phen) 3 (mal)] Æ 2H2O,[Cu (phen) 2 (mal)] Æ 2H2O and [Mn (phen) 2 (mal)] Æ 2H2O (malH2= malonic acid) using human cancer cells; Cancer Lett.; 2007, **247**, 224.

xi Fan L.; Tian M.; Liu, Y.; Deng, Y.; Liao, Z.; Xu J.; Salicylate-Phenanthroline copper (II) complex induces apoptosis in triple-negative breast cancer cells;Oncotarget; 2017, **8**(18), 29823.

xii Zhen N.; Yang Q.; Wu Q.; Zhu X.; Wang Y.; Sun F.; Yu Y.; A novelly synthesized phenanthroline derivative is a promising DNA-damaging anticancer agent inhibiting G1/S checkpoint transition and inducing cell apoptosis in cancer cells; Cancer Chemother. Pharmacol.; 2016, **77**, 169.

xiii Upadhyay, A.; Gautam, S.; Ramu, V.; Kondaiah P.; Chakravarty A.; Photocytotoxic cancer cell-targeting platinum (II) complexes of glucose-appended curcumin and biotinylated 1, 10-phenanthroline. Dalton Trans.; 2019, **48**(47), 17556-17565.

xiv Ünver H.; Berber B.; Kanat B., Arafat M.; Koparal A.; Doluca O.; DNA binding effects of 2, 2′-bipyridine and 1, 10-phenanthroline ligands synthesized with benzimidazole copper (II) complexes: Crystal structure, molecular docking, DNA binding and anti-cancer studies; Polyhedron, 2022, **221**, 115834.

xv Al-Matarneh C.; Amarandi R.; Craciun A.; Mangalagiu I.; Zbancioc G.; Danac, R.; Design, synthesis, molecular modelling and anticancer activities of new fused phenanthrolines; Molecules, 2020, **25**(3), 527.

xvi Zhang Z.; Wang H.; Wang Q.; Yan M.; Wang H.; Bi C.; Fan Y.; Anticancer activity and computational modeling of ternary copper (II) complexes with 3-indolecarboxylic acid and 1, 10-phenanthroline; International J. Oncol.; 2016, **49**(2), 691-699.

xvii Figueroa-Valverde L.; Rosas-Nexticapa M.; Montserrat M.; Díaz-Cedillo F.; López-Ramos M.; Alvarez-Ramirez M.;. Synthesis and Theoretical Interaction of 3-(2-oxabicyclo [7.4. 0] trideca-1 (13), 9, 11-trien-7-yn-12-yloxy)-steroid Derivative with 17β-hydroxysteroid Dehydrogenase Enzyme Surface; Biointerface Res. Appl. Chem.; 2023, **13**, 266.

xviii Sizemore N.; Heil E.; Computational analysis of intermolecular Diels–Alder reactions of methyl 2-(methyl (phenyl) carbamoyl) acrylate with cyclic dienes. J. Pennsylvania Acad. Sci.; 2019, **93**(2), 118.

xix Lopez-Ramos M.; Figueroa-Valverde L.; Diaz-Cedillo F.; Rosas-Nexticapa M.; Alvarez-Ramirez M.; Theoretical Evaluation of Twenty-Cannabinoid Derivatives on Either Androgen Receptor or 5α-Reductase Enzyme; Clin. Cancer Invest. J.; 2023, **12**(2), 27-32,

xx Rosas-Nexticapa M.; Figueroa-Valverde L.; Alvarez-Ramirez M.; Lopez-Ramos M.; Mateu-Armand V.; Lopez-Gutierrez, T.; Evaluation of Interaction of Some Quinolone Derivatives on RSK-4 Using a Theoretical Model; Clin. Cancer Invest. J.; 2022, **11**(6), 16.

xxi Toure O.; Dussap C.; Lebert A.; Comparison of predicted pKa values for some amino-acids, dipeptides and tripeptides, using COSMO-RS, ChemAxon and ACD/LABS methods; Rev. IFP Energ. Nouv.; 2013, **68**(2), 281.

xxii Al-Hageh C.; Al-Assaad M.; El-Masri Z.; Samaan N.; El-Sibai M.; Khalil C.; Khnayzer R.; A long-lived cuprous bis-phenanthroline complex for the photodynamic therapy of cancer; Dalton Trans.; 2018, **47**(14), 4959.

xxiii Deegan C.; McCann M.; Devereux M.; Coyle B.; Egan D.; In vitro cancer chemotherapeutic activity of 1, 10-phenanthroline (phen),[Ag2 (phen) 3 (mal)] Æ 2H2O,[Cu (phen) 2 (mal)] Æ 2H2O and [Mn (phen) 2 (mal)] Æ 2H2O (malH2= malonic acid) using human cancer cells; Cancer Lett.; 2007, **247**, 224.

xxiv Laws K.; Bineva-Todd G.; Eskandari A.; Lu C.; O'Reilly N.; Suntharalingam K.; A copper (II) phenanthroline metallopeptide that targets and disrupts mitochondrial function in breast cancer stem cells. Angew. Chem.; 2018, **130**(1), 293.

xxv Osei P.; Northcote-Smith J.; Fang J.; Singh K.; Ortu F.; Suntharalingam K.; The Bulk Breast Cancer Cell and Breast Cancer Stem Cell Activity of Binuclear Copper (II)-Phenanthroline Complexes; Chemistry-A Eur. J.; 2023, **29**(45), e202301188.

xxvi Wolber G.; Kosara, R.; Pharmacophores from macromolecular complexes with LigandScout; Pharmacophores Pharm. Sear.; 2006, **32**, 131.

xxii Alamri M.; Alamri M.; Pharmacophore and docking-based sequential virtual screening for the identification of novel Sigma 1 receptor ligands. Bioinf.; 2019, **15**(8), 586.

xxviii Vuorinen A, Engeli R, Meyer A, Bachmann F, Griesser U. Schuster D. Odermatt A. Ligand-based pharmacophore modeling and virtual screening for the discovery of novel 17β-hydroxysteroid dehydrogenase 2 inhibitors; J. Med. Chem.; 2014, **57**(14), 5995.

xxix Khan H.; Kulsoom S.; Rashid H.; Ligand based pharmacophore model development for the identification of novel antiepileptic compound; Epilepsy Res.; 2012, **98**(1), 62.

xxx Lewis D.; Frontier orbitals in chemical and biological activity: quantitative relationships and mechanistic implications; Drug Met. Rev.; 1999, **31**(3), 755.

xxxi Henkels K.; Farkaly T.; Mahankali; M.; Segall; J.; Gomez-Cambronero J.; Cell invasion of highly metastatic MTLn3 cancer cells is dependent on phospholipase D2 (PLD2) and Janus kinase 3 (JAK3); J. Mol. Biol.; 2011, **408**(5), 850.

xxxii Koo G.; Tan S.; Tang T.; Poon S.; Allen G.; Tan L.; Lim S.; Janus kinase 3-activating mutations identified in natural killer/T-cell Lymphoma; Cancer Dis.; 2012, **2(**7), 591.

xxxiii Sudbeck E.; Liu X.;Narla R.; Mahajan S.; Ghosh S.; Mao C.; Uckun F.; Structure-based design of specific inhibitors of Janus kinase 3 as apoptosis-inducing antileukemic agents; Clin. Cancer Res.; 1999, **5**(6), 1569.

xxxiv Genovese M.; Van-Vollenhoven R.; Pacheco-Tena C.; Zhang Y.; Kinnman N.; VX-509 (Decernotinib), an oral selective JAK-3 inhibitor, in combination with methotrexate in patients with rheumatoid arthritis; Arth. Rheum.; 2016, **68**(1), 46.

xxxv Bezzio C.; Vernero M.; Ribaldone D.; Alimenti E.; Manes G.; Saibeni, S.; Cancer Risk in Patients Treated with the JAK Inhibitor Tofacitinib: Systematic Review and Meta-Analysis; Cancers, 2023, **15**(8), 2197.

xxxvi Alvarez-Ramirez M.; Figueroa-Valverde L.; Diaz-Cedillo F.; Rosas-Nexticapa M.; Lopez-Ramos M.; Mateu-Armand V.; Theoretical Evaluation of Furanone and its Derivatives for the Treatment of Cancer Through Eag-1 Inhibition; Clin. Cancer Invest. J.; 2023, **12**(4), 4.

xxxvii Perozzo R.; Folkers G.; Scapozza L.; Thermodynamics of protein-ligand interactions: history, presence, and future aspects; J. Rec. Sign.Trans.; 2004, **24**(1-2), 1.

xxxviii Olsson T.; Williams M.; Pitt W.; Ladbury J.; The thermodynamics of protein-ligand interaction and solvation: insights for ligand design; J. Mol. Biol.; 2008, **384**(4), 1002.

Received on March 5, 2024.